https://doi.org/10.5194/egusphere-2024-2634
Preprint. Discussion started: 27 August 2024

Investigating the influence of changing ice surfaces on gravity wave formation and glacier boundary-layer flow with large-eddy simulations

Brigitta Goger[1,2], Lindsey Nicholson[2], Matthis Ouy[2], and Ivana Stiperski[2]

[1]Center for Climate Systems Modeling, ETH Zurich, Zurich, Switzerland
[2]Department of Atmospheric and Cryospheric Sciences, Universtität Innsbruck, Innsbruck, Austria

Correspondence: Brigitta Goger (brigitta.goger@c2sm.ethz.ch)

Abstract. Mountain glaciers are located in highly complex terrain and their local micro-climate is influenced by mountain boundary layer processes and dynamically-induced gravity waves. Observations (turbulence flux towers) and simulations (large-eddy simulation) over the Hintereisferner (HEF) glacier in the Austrian Alps have shown that down-glacier winds are often disturbed by cross-glacier flow from the North-West associated with gravity waves. In this work, we explore how the glaciers located upstream of HEF influence the gravity wave formation and intensity and and the feedback this has on boundary layer flow over HEF. In semi-idealized large-eddy simulations, we explore the impact of changing surface properties on HEF's microclimate by removing the upstream glaciers only (NO_UP) and removing all ice surfaces (NO_GL). Simulations suggest that removing the upstream glaciers (which causes a change of boundary layer stratification from stable to unstable) leads to a weaker gravity wave breaking earlier than in the reference simulation and leading to enhanced turbulent mixing over HEF. As a consequence, this results in higher temperatures, sensible heat fluxes, and stronger warm-air advection over HEF tongue. Removing all glaciers results - as expected - in higher temperatures of up to 5 K over the missing ice surfaces, while the gravity wave pattern is similar as in the NO_UP simulation, indicating that the upstream boundary layer exerts dominant control over downstream response in such highly dynamic conditions. This study shows that a single glacier tongue is never isolated from its environment and that surrounding glaciers and local topography have to be taken into account when studying glacier boundary-layer processes. Furthermore, glaciers have a stabilizing effect on the boundary layer, impacting gravity wave formation and downslope windstorm intensity and their impact on the flow structure in valleys downstream.

1 Introduction

The Earth's mountainous regions are important sources for global freshwater resources, and are being strongly affected by climate change and elevation-dependent warming (Hock et al., 2022; Byrne et al., 2024). In recent years, the European mountain cryosphere (permafrost, glaciers, snow) is experiencing significant changes (Beniston et al., 2018) with decreasing overall snow depths (Matiu et al., 2021) and rapid and accelerating glacier recession (e.g., Voordendag et al., 2023; Cremona et al., 2023). While there is a clear scientific consensus on the large-scale patterns of glacier recession, there is still a knowledge gap

https://doi.org/10.5194/egusphere-2024-2634
Preprint. Discussion started: 27 August 2024

on how glacier shrinkage influences the mountain boundary layer and how that in turn will influence subsequent glacier melt (Beniston et al., 2018).

The mountain boundary layer (MoBL) forms due to complex interactions between heterogeneous, complex topography and the atmosphere aloft on timescales of less than an hour (Rotach and Zardi, 2007; Lehner, 2024). One of the major features of the MoBL are thermally-induced circulations at several scales, from slope flows over valley winds up to Alpine pumping (Zardi and Whiteman, 2013; Goger and Dipankar, 2024) influencing the exchange of heat, mass, and momentum between the free atmosphere and the surface. European glaciers are located in mountainous terrain, and although they develop their own micro-climate with katabatic down-glacier flows, they are also affected by valley winds or the larger-scale synoptic flow (Oerlemans, 2010). For example, observations over Breidamerkurjökull, Iceland, show that the katabatic glacier boundary layer flow is mostly undisturbed even by storms (Parmhed et al., 2004). On a glacier in the Alps, however, Litt et al. (2017) suggest that under strong synoptic forcing, the large-scale flow disturbs the glacier boundary layer and no katabatic signal is detectable. During the FLOHOF campaign over Hofsjökull glacier, Iceland, gravity waves induced pressure perturbations between -2 hPa and 2 hPa in the glacier boundary layer (Reuder et al., 2012; Egger and Kühnel, 2010). Gravity waves are common over the Alps (Jiang and Doyle, 2004) and are a well-known phenomenon in mountain meteorology that interact on various scales within the stable boundary layer (Vosper et al., 2018). Therefore, gravity waves are among the dynamically-induced processes over complex terrain frequently interacting with valley and glacier boundary layers (Finnigan and Einaudi, 1981; Lott, 2016), and they influence glacier-atmosphere exchange especially during summer on snow-free glacier surface (Nicholson and Stiperski, 2020). Under a changing climate, recent observations and modelling over the Haut d'Arolla glacier in the Swiss Alps suggest that with a decreasing glacier ice area the thermally-induced up-valley flow progressively dominates the glacier micro-climate and ultimately might contribute to increased melting (Shaw et al., 2023, 2024). Besides the aforementioned localized studies, observations by Conway et al. (2021) in the Canadian Rockies suggest that local glacier boundary-layer flow is also influenced by local breeze systems ("Icefield breezes"), and that a single glacier tongue might not be isolated from its environment.

During the Hintereisferner Experiment (HEFEX, Mott et al., 2020), along- and across-glacier transects of eddy-covariance (EC) stations were employed at the Hintereisferner (HEF) glacier, Austrian Alps. This allowed an analysis of spatial heat advection patterns and mostly cold-air advection was found on the glacier during down-glacier katabatic winds. However, the katabatic glacier wind was often disturbed by lateral (cross-glacier) flow associated with warm-air advection. Within the HEFEX observational setup, the reason for these disturbances could not be immediately identified; and one of the major questions was the origin of the cross-glacier flow and whether the presence of nearby glaciers have a strong impact on the cross-glacier flow formation. High-resolution large-eddy simulations have emerged as a useful tool for process understanding over complex terrain (e.g., Heinze et al., 2017; Gerber et al., 2018; Kiszler et al., 2023; Sauter and Galos, 2016; Voordendag et al., 2024; Omanovic et al., 2024; Draeger et al., 2024) and a large-eddy simulation (LES) setup has been used to investigate the nature and source of cross-glacier disturbances in the HEFEX campaign (Goger et al., 2022). With a horizontal mesh size of 48 m, the LES are able to simulate the relevant mesoscale flow structures and wind patterns on the glacier for both summer and winter (Goger et al., 2022; Voordendag et al., 2024).

https://doi.org/10.5194/egusphere-2024-2634
Preprint. Discussion started: 27 August 2024

Two case studies with two different flow directions were conducted, and it was found that under North-Westerly synoptic winds a gravity wave forms upstream of HEF. The gravity wave in the Goger et al. (2022) LES case study was associated with warm-air advection over the glacier tongue in agreement with the observations. However, the role of the upstream glaciers on these cross-glacier "disturbances" remains is not clear. Gravity wave formation depends on the topography shape, the upstream profile of wind speed, and the stability (Jackson et al., 2013). The upstream glaciers present a surface with very specific characteristics compared to ice-free terrain. The melting glaciers during summer daytime exhibit a constant surface temperature of 0^{deg}C, and their surface roughness differs strongly from ice-free areas. At the same time, glaciers present a comparatively smoother surface than ice-free mountainous areas. Thus the effect of removing upstream glaciers manifests itself in the change of surface roughness as well as boundary layer type (stable over ice surface and unstable during daytime over ice-free surfaces) and the associated potential temperature and wind speed structure. In a study of foehn flow over the Larsen C ice shelf, Antarctica, Turton et al. (2018) hypothesize that upstream ice surfaces influence the isentrope downdraw in downslope windstorms. A numerical sensitivity study over Hofsjökull ice cap, Iceland, suggests that downslope windstorms are stronger due to the ice surfaces, while removing the icecap from the simulation domain led to weaker gravity waves (Jonassen et al., 2014), where the authors attribute this change mostly to changed surface roughness with a minimal effect of temeprature change.

At Hintereisferner glacier, we continue the study from Goger et al. (2022) and remove the upstream glaciers in a semi-idealized setup for a case study day and pose the following research questions:

- What is the impact of the upstream glaciers on gravity wave formation and on the resulting cross-glacier flow over HEF?
- What is the overall impact of removing upstream ice surfaces on the boundary layer development over HEF and how are surface exchange and temeprature patterns affected?
- What is the impact of deglaciation on the valley boundary layer and surface exchanges?

To anser whtese questions, we organize this paper as follows: In Section 2, we describe the area of interest and our model set-up. Section 3 describes the impact of the changing ice surfaces on the wind structure and upstream profiles, followed by Section 4, where we discuss the impact of the missing upstream glaciers on the sensible heat fluxes and temperatures on the (remaining) glacier, before we discuss the results and conclude.

2 Location of interest and numerical simulations

2.1 The Hintererisferner (HEF) glacier

We are interested in the Hintereisferner (HEF), a large valley glacier in the Ötztal Alps, Austria. In 2018 (the year of our case study), HEF was around 6.3 km long, decending from its highest point, Weißkugel (3738 m asl), to 2460 m asl, where the glacier tongue terminates. The glacier has been subject to continuous mass balance monitoring and meteorological observations for more than 150 years (Obleitner, 1994; Strasser et al., 2018) and is one of the benchmark glaciers of the World glacier

https://doi.org/10.5194/egusphere-2024-2634
Preprint. Discussion started: 27 August 2024

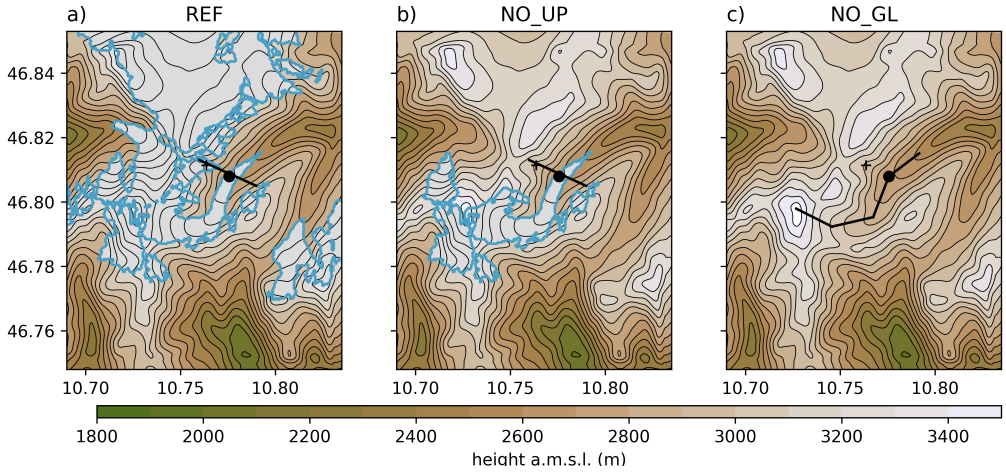

Figure 1. Overview of the model topography of the innermost domain (color contours) and the glacier outlines in light blue for (a) the reference run with realistic glacier outlines (REF), (b) no upstream glaciers (NO_UP), and (c) without glaciers (NO_GL). The black lines show the cross-section lines, the black dot shows the location "HEF tongue", and the black plus shows the location "upstream".

monitoring network (WGMS, 2017). The glacier is, as the rest of the European mountain cryosphere (Beniston et al., 2018), affected by persistent and accelerating mass loss since the 1980's. While it loses around 1 m ice thickness per year over the last 20 years(Piermattei et al., 2024), extreme mass loss has been observed in some recent years (Voordendag et al., 2023). The HEFEX campaign took place on the glacier in the summer of 2018, with an array of EC stations placed on the glacier tongue (Mott et al., 2020), revealing among the expected katabatic down-glacier flow also frequent intrusions from the North-West, leading to an erosion of the glacier boundary layer. These disturbances were investigated with numerical simulations by Goger et al. (2022), revealing gravity waves over the North-Western ridge to be the major mechanism behind the intrusions into the katabatic flow.

2.2 Numerical model

We employ the Weather Research and Forecasting (WRF) model version 4.1 (Skamarock et al., 2019) for our numerical study. Most of the model set-up is similar to Goger et al. (2022), therefore we only repeat the most relevant information for our present study. We use a nested set-up consisting of four domains, where the outermost domain spans Europe with Δx=6 km and receives ERA5 input data (Hersbach et al., 2020) as boundary and initial conditions. We subsequently nest down over Δx=1 km, and Δx=240 m to the innermost domain at Δx=48 m. We use the Thompson microphysics (Thompson et al., 2008), the MM5 revised surface layer scheme (Jiménez et al., 2012), and the RRTMG two-stream radiation scheme (Iacono et al., 2008) with topographic shading for all domains. We switch off the boundary layer parameterization in the two innermost domains and employ the turbulence closure after Deardorff (1980). Since the boundary-layer flow is of turbulent nature, we utilize the online averaging module "WRF LES diagnostics" by Umek (2020) and create 15-minute averages of selected model

https://doi.org/10.5194/egusphere-2024-2634
Preprint. Discussion started: 27 August 2024

variables. All simulations were initialized on Aug 17, 03:00 UTC and ran for 18 hours. Test simulations from Goger et al. (2022) suggest that the first three hours of simulation have to be regarded as spin-up time, and therefore we will analyze the model output for the time period of 06:00 UTC until 12:00 UTC to allow direct comparison to the reference simulation, which delivered most reliable results during this time period according to a validation with observations (Goger et al., 2022). In this study, we only show the output domain 4 for our analysis, and any mentioned numerical data will stem from this domain at Δx=48 m.

The run with the realistic glacier surfaces from 2018 (NW flow, Goger et al., 2022) will serve as the reference run (REF, Fig. 1a). We conduct two extra sensitivity runs of domain 3 (Δx=240 m) and domain 4 (Δx=48 m) with changes in glacier ice surfaces: For the first sensitivity run, we remove the upstream glaciers North of HEF (NO_UP, Fig. 1b), while for the second sensitivity run, we remove all glacier surfaces, including HEF, from the domain (NO_GL, Fig. 1c). At this point, we want to mention that the two sensitivity runs do not represent realistic glacier surfaces under future climate projections (Zekollari et al., 2019), because the projections predict a continuous shrinkage of all ice surfaces instead of removing the entire upstream glaciers as in our NO_UP run. Furthermore, real world glacier recession progresses from lower to higher elevations, while our case study involves the unrealistic removal of high elevation ice surrounding HEF. However, the aim of this study is not to investigate the glacier boundary layer development under future climate scenarios, but rather to explore to role of the upstream glaciers on the local boundary layer over HEF and the associated surface exchange. Compared to the REF run where a stable boundary layer is present over all ice surfaces upstream of HEF and thus impacts the gravity wave, in the NO_UP and NO_Gl simulations, a convective boundary layer can develop thus affecting the flow. Therefore, we see the NO_UP and NO_GL runs as "semi-idealized" simulations. As outlined in the introduction, we choose August 17, 2018 as a case study day, because the synoptic flow direction was mostly North-Westerly disturbing the small-scale glacier boundary layer (Goger et al., 2022, their NW day case study).

3 Wind patterns and upstream flow structure

The reference simulation (REF) is a real-case simulation of the glacier boundary layer from August 17, 2018. Under North-Westerly synoptic influence, a gravity wave formed over the North-Western ridge close to HEF, leading to a continuous disturbance of the glacier boundary layer. The model suggested mostly cross-glacier flow and high values of non-stationarity of the sensible heat flux with a strong mesoscale influence on the glacier boundary layer. Details on the simulation and further results can be found in Goger et al. (2022), their "NW day". In the following sections, we describe two further simulations exploring the impact of removing the upstream glaciers (NO_UP) and of removing all ice surfaces in the domain altogether (NO_GL) on gravity waves and local boundary layer development. We will investigate the time period from 06:00 UTC until 12:00 UTC, because REF delivered most reliable results in comparison with observations from the HEFEX campaign during this time period (Goger et al., 2022). After 12:00 UTC, the simulation started to deviate, especially in terms of wind speeds, from the observed values; to keep a fair comparison to REF, we will also only analyse the 6 hours of simulation time in NO_GL and NO_UP.

https://doi.org/10.5194/egusphere-2024-2634
Preprint. Discussion started: 27 August 2024

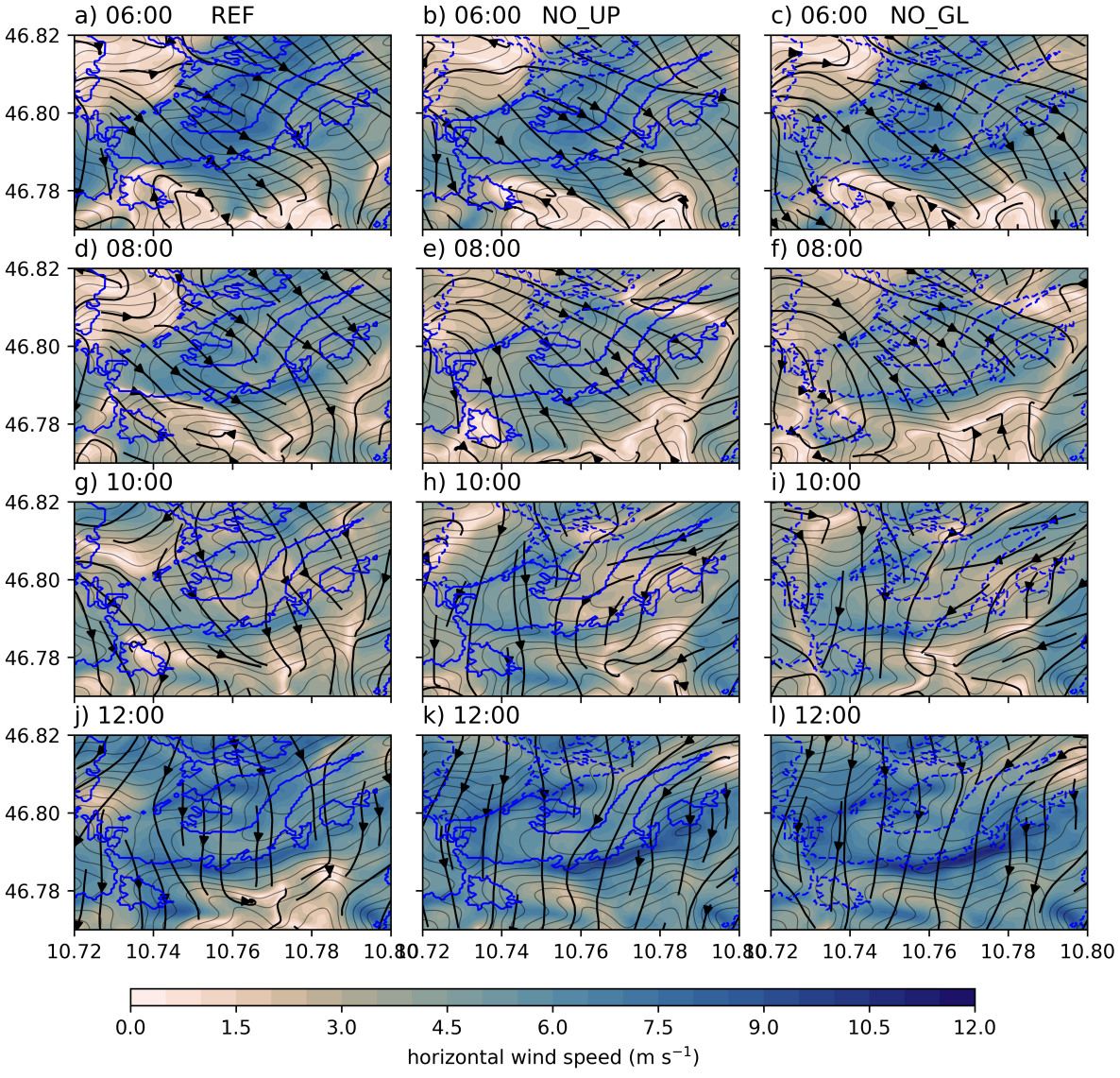

Figure 2. Simulated horizontal wind speed (colors) from the lowest model level and streamlines (black arrows) at four different times (06:00 UTC, a-c; 08:00 UTC, d-e; 10:00 UTC, g-i; 12:00 UTC, j-i). Left row: REF; middle: NO_UP, right row: NO_GL. The blue contours represent the glacier outlines in the simulations, while dashed blue lines in the middle row indicate the 'missing' ice surfaces. The thin black contours show model topography.

3.1 Spatial patterns of the wind field

A comparison of horizontal wind speeds from the lowest model level between the REF, NO_UP and NO_GL simulations reveals differences in the flow structure over the glacier dependent on time of the day (Fig 2). In the morning (06:00 UTC,

https://doi.org/10.5194/egusphere-2024-2634
Preprint. Discussion started: 27 August 2024

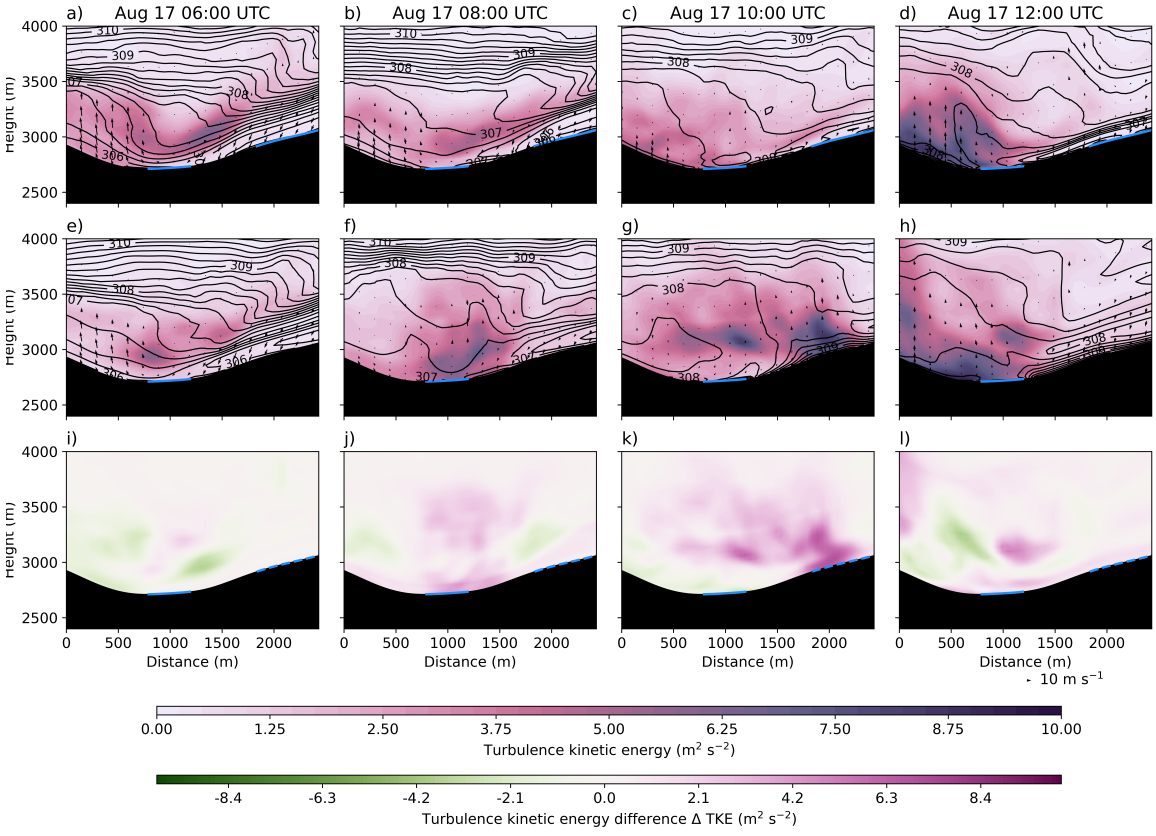

Figure 3. Vertical cross-section along the black line in Fig. 1b of simulated total TKE (subgrid + resolved, colors), isentropes (black contours), and cross-valley wind speed (arrows) from the REF simulation (panels a-d), the NO_UP simulation (panels e-h) and the difference in TKE of NO_UP-REF (panels (i-l).

Fig 2a-c), cross-glacier flow with wind speeds of around 6 m s^{-1} dominates in all three simulations. In the REF simulation, this cross-glacier flow is present throughout the simulation. In the NO_UP and NO_GL simulations, however, we note the weakening of the cross-glacier flow after 08:00 UTC (Fig 2e,f). While the cross-glacier flow prevails with reduced wind speeds in the REF simulation at 10:00 UTC (Fig 2g), the NO_UP and NO_GL simulations show an up-glacier flow dominating the wind field at the glacier tongue (Fig 2h,i). This up-glacier flow persists until 12:00 UTC (Fig 2k,l), together with a horizontal wind speed maximum at the North-facing slope next to the glacier. In the next paragraphs, we will explore the nature and origin of the up-glacier flow in the two simulations without the upstream glaciers.

3.2 Vertical structure of the upstream flow

To better understand the wind patterns and the reasons for the up-glacier flow in the NO_UP and NO_GL simulations, we examine the vertical structure of the upstream flow conditions in the next paragraphs.

https://doi.org/10.5194/egusphere-2024-2634
Preprint. Discussion started: 27 August 2024

Although the surface flow showed similar characteristics between the different simulations at 6 UTC, vertical cross-section shows some marked differences. In the REF simulation, the cross-section of steepening isentropes at around 3500 m above mean sea level in the HEF valley at 06:00 UTC reveals a gravity wave with hydraulic jump-like features (Fig. 3a), with an elevated turbulence kinetic energy (TKE) maximum around 200 m above the surface. At the same time in the NO_UP simulation (Fig. 3e), the general structure of the gravity wave is similar to REF, but with already overturning isentropes, indicating wave breaking, associated with reduced stability and a weaker TKE maximum (-5 $m^2\ s^{-2}$) that is more in the valley central flowline than in REF (Fig. 3i). Two hours later (08:00 UTC), the gravity wave overturns in the REF simulation as well (Fig. 3b), while the gravity wave in NO_UP simulation already broke, with reduced upstream stability under the influence of and increase of surface friction (Fig. 3f) and strong turbulent mixing over HEF tongue with higher TKE values than REF (Fig. 3j). At 10:00 UTC, the gravity wave in REF also breaks (Fig. 3c), while NO_UP shows no distinct gravity wave pattern anymore in the isentropes (Fig. 3g) with strong turbulent mixing and higher TKE values are present over HEF tongue (Fig. 3k). At 12:00 UTC, the highest TKE values are simulated over the glacier by the REF simulation, and the gravity wave re-established with shooting downslope flow, while in the NO_UP simulation, reduced stability is visible upstream in association with a much weaker gravity wave (Fig. 3h) and reduced TKE values (Fig. 3j). To summarize, a gravity wave is present in both simulations over the glacier valley. However, in the NO_UP simulation, the gravity wave is weaker with a different breaking pattern, leading to higher TKE values and enhanced mixing over the glacier tongue. In the NO_GL simulations, the general structure and gravity wave formation as similar as in the NO_UP simulation (not shown). Therefore, we conclude that most of the gravity wave's dynamics is governed by the upstream glacier and not by HEF itself.

To further explore how the upstream profiles influencing gravity wave formation, we show vertical profiles of potential temperature, wind speed, wind direction, and the Scorer parameter from HEF tongue and from a point upstream in Fig. 4. The Scorer parameter is defined as

$$l^2(z) = \frac{N^2}{U^2} - (\frac{\partial^2 U}{\partial z^2})/U \tag{1}$$

where $N = N(z)$ is the Brunt-Väisälä frequency dependent opn the height z, and $U = U(z)$ is the vertical profile of the horizontal wind. When $l^2(z)$ decreases or changes strongly with height, conditions are favorable for the formation of trapped lee waves, forming with stable boundary layers below an inversion and lower static stability aloft (Scorer, 1949). The Scorer parameter is also useful to explore flows over glaciated areas to identify wave trapping in katabatic flows (Parmhed et al., 2004; Söderberg and Parmhed, 2006).

At 06:00 UTC, the potential temperature profile at HEF tongue reveals a stable boundary layer (Fig. 4a) in all simulations at both locations (HEF tongue and upstream), in accordance with a weak down-glacier jet (Fig. 4b). The only difference between REF and the simulations without the upstream glaciers is the location of the jet maximum. At the upstream location, we find stable stratification in the potential temperature profiles in all simulations and already North-Westerly flow. The Scorer parameter (Fig. 4i) shows mostly local maxima close to the inversions (cf. Fig. 4a) except for one large decrease in the REF simulation at the upstream location. Two hours later, differences start to emerge between the simulations: At HEF tongue, we note that higher potential temeprature values by 2 K in NO_UP and NO_GL compared to REF (cf. Fig. 4b). At the upstream

https://doi.org/10.5194/egusphere-2024-2634
Preprint. Discussion started: 27 August 2024

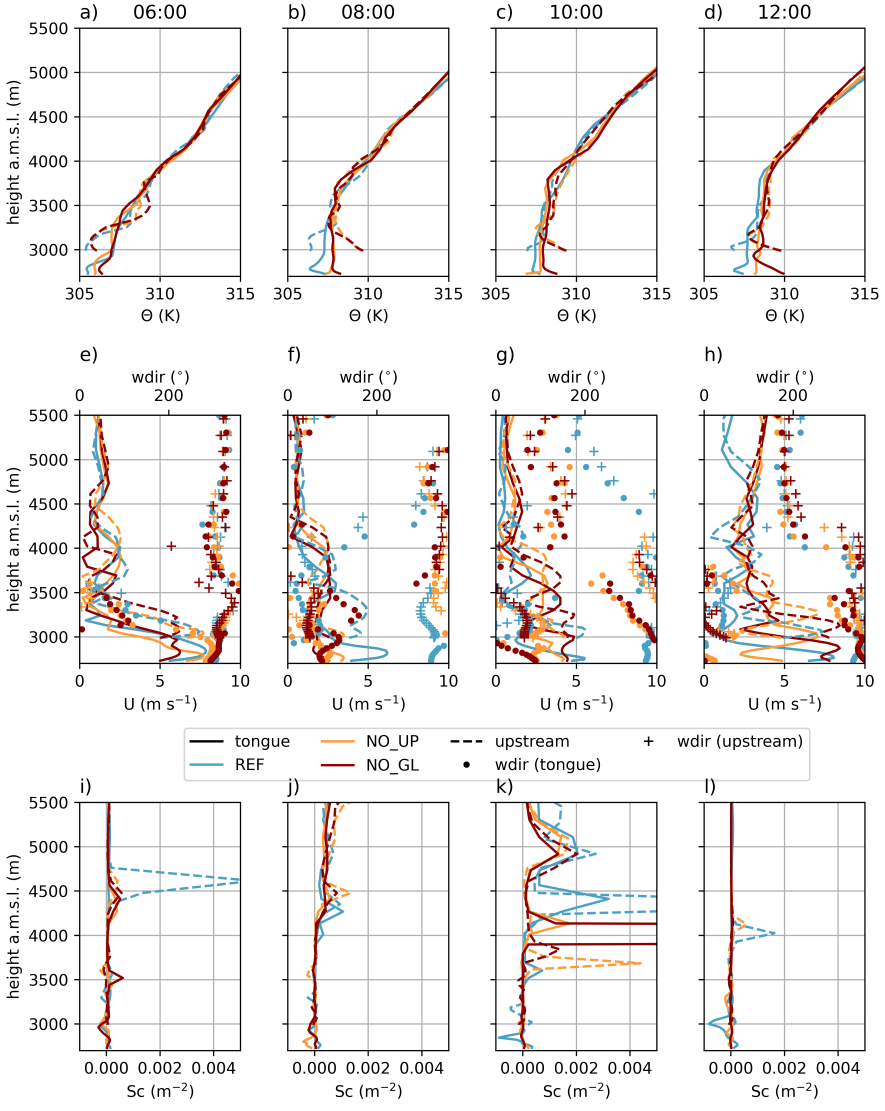

Figure 4. Vertical Profiles of potential temperature (panels a-d), horizontal wind speed and direction (panels e-h), and the Scorer parameter (panels i-l) from REF (blue), NO_UP (orange), and NO_GL (red) from two locations ("HEF tongue", full lines; and "Upstream", dashed lines) from four times.

location, this potential temperature difference is even higher by up to 4 K, and the profiles in the simulations without the upstream glaciers now show unstable stratification (and a convective boundary layer) compared to the stable stratification in the REF simulation. The wind speeds show a less distinct jet in the simulations without the upstream glaciers, while there is still a distinct low-level jet maximum in REF over HEF tongue (cf. Fig. 4f). The Scorer parameter shows almost no favorable
190 conditions for gravity wave formation, in accordance with the weakened gravity wave visible in the cross-sections at 08:00 UTC

https://doi.org/10.5194/egusphere-2024-2634
Preprint. Discussion started: 27 August 2024

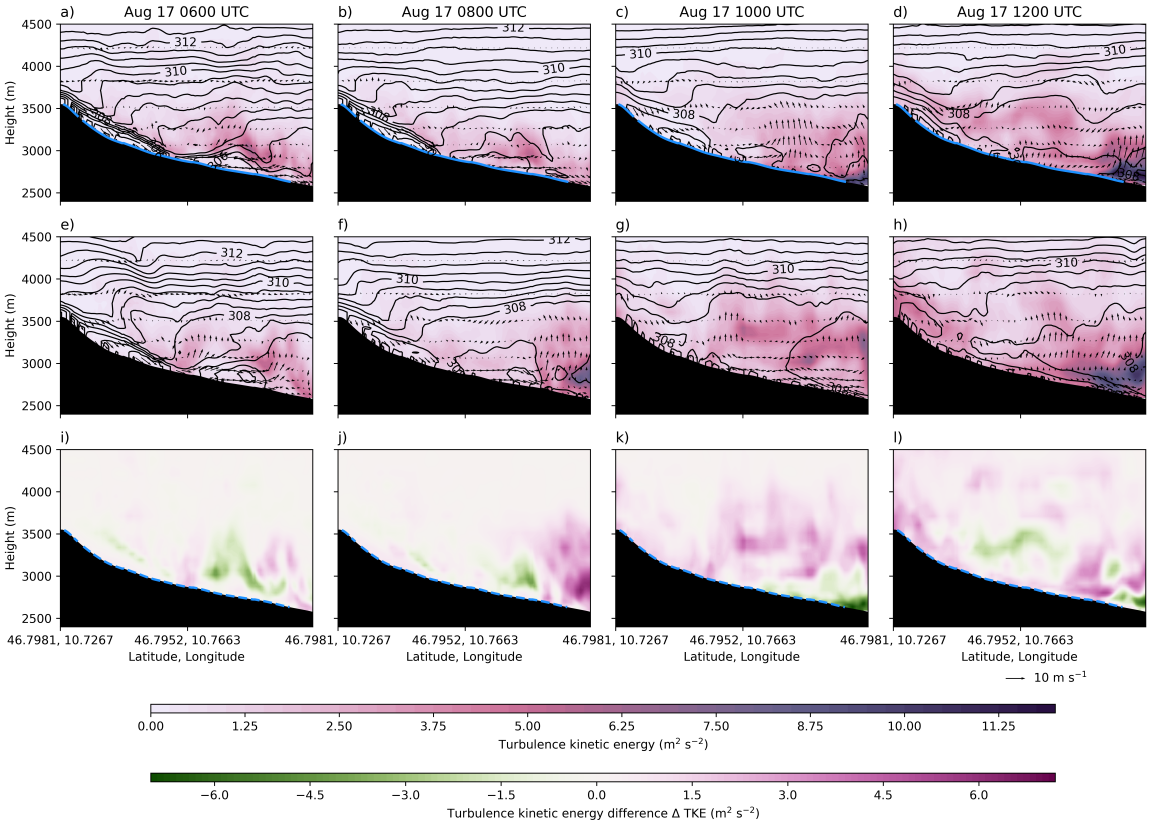

Figure 5. Vertical cross-section along the line in Fig. 1c of simulated total TKE (colors), isentropes (black countours), and along-valley wind speed (arrows) from the REF simulation (panels a-d), the NO_GL simulation (panels e-h) and the difference in TKE in NO_UP-REF (panels (i-l).

(cf. Fig. 3b,f). At 10:00 UTC, the potential temperature profiles (cf. Fig. 4c) show a similar picture as at 08:00 UTC at both locations. However, the wind direction now reveals a distinct up-valley flow in the NO_UP and NO_GL simulations (Fig. 4g), while the flow remains cross-glacier in the REF simulation, while the upstream flow direction remain North-Westerly in all simulations. The Scorer parameter again shows favorable conditions for gravity wave formation, while they are strongest in the REF simulation (Fig. 4k). Finally, at 12:00 UTC, there are clear differences in the potential temperature profiles: At HEF tongue, we note a convective boundary layer in NO_GL, while there is mostly neutral stratification in REF and NO_UP (Fig. 4d). Upstream, there is still stable stratification in REF, while the simulations wihtout the upstream glaciers show neutral or convective boundary layers. The wind patterns (Fig. 4h) show a chaotic behaviour, due to the gravity wave breaking and strong turbulence (cf. Fig. 3), while it is clear that the synoptic flow from aloft changes direction at heights below crest height: All simulations show now an up-glacier flow. The Scorer parameter agin reveal no signs favorable for gravity wave formation (Fig. 4l).

https://doi.org/10.5194/egusphere-2024-2634
Preprint. Discussion started: 27 August 2024

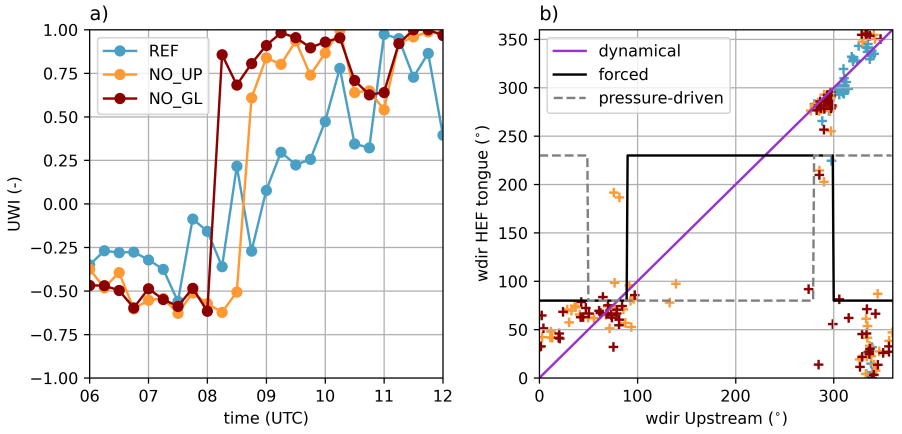

Figure 6. Panel a) UWI for REF, NO_UP, and NO_GL for the location HEF tongue. Panel b) Scatter plot of wind direction (+) at locations 'Upstream' and at 'HEF tongue' for all three simulations for our time period of interest. The lines in purple, black, andgrey show the idealized categorizations from Whiteman and Doran (1993).

Since we noted a distinct up-valley flow in the simulations without the upstream glaciers (NO_UP and NO_GL), we explore the vertical structure of the atmosphere along the glacier (Fig. 5) as well.

The REF simulation exhibits at 06:00 UTC a strong stable boundary layer (SBL) at the upper parts of the glacier (Fig. 5a) and a down-glacier flow, and reduced stability and higher TKE values at the lower part. In NO_GL, there is a neutral layer with a weaker inversion aloft (Fig. 5e) and generally weaker stratification and lower TKE values (Fig. 5i). Two hours later, the SBL over the upper part of HEF is still present in REF, while it is now much weaker in NO_GL. Furthermore, NO_GL exhibits higher TKE values than REF at the lower part, related to the earlier breaking cross-glacier gravity wave. at 10:00 and 12:00 UTC (Fig. 5c,d,g,h), the atmosphere above HEF is well-mixed in both REF and NO_GL. In REF, the SBL is still noticeable in upper parts, but it dissipated in the NO_GL simulations. This might be one of the major reasons why the gravity wave is able to plunge and break into the glacier valley earlier in the NO_GL and NO_UP simulations than in REF, because there is a weaker (or no) cold-air pool which has to be eroded by the upper-level flow (Haid et al., 2022). Furthermore, the up-glacier flow is also noticeable in the NO_GL simulations with enhanced turbulent mixing. At this point, it is not clear which kind of forcing (thermally- or dynamically-induced) leads to the distinct up-glacier flow in the NO_GL and NO_UP simulations, therefore we will explore the origin of the up-glacier flow in the next section.

3.3 Wind direction shift in the glacier valley

In the following paragraphs, we disentangle the dynamical mechanisms related to the change of the wind direction from cross-glacier to up-glacier in the simulations without the upstream glaciers. Shaw et al. (2023) developed an "up-valley wind index" (UWI) based on the wind direction

$$UWI = cos(\frac{|wdir - \phi|\pi}{180}) \quad (2)$$

https://doi.org/10.5194/egusphere-2024-2634
Preprint. Discussion started: 27 August 2024

where $wdir$ is the wind direction at 10 m above ground at HEF tongue, and ϕ is the orientation of the glacier valley (in our case 45°). When $UWI = 1$, the flow is exactly up-glacier, while $UWI \approx 0 - 0.5$ indicates cross-glacier flow. In our simulations, the flow is cross-glacier for all three cases (Fig. 6a) before 08:00 UTC, related to the gravity wave present over the glacier tongue. However, after 08:00 UTC, the situation changes: In REF, there is a gradual shift in UWI towards 1 until 12:00 UTC, suggesting a gradual weakening of the cross-glacier flow associated with the gravity wave. However, in the other two simulations, UWI shows a sudden shift towards 1 already at 08:00 UTC (NO_GL) and 08:30 (NO_UP), suggesting up-glacier flow. When the gravity wave breaks (cf. Fig. 3, at 10:00 UTC), the up-valley flow can develop (cf. Fig. 2) and, in contrast to the REF simulation, the gravity wave is unable to re-develop and the up-glacier flow persists after 09:00 UTC in NO_UP and NO_GL.

However, the UWI only gives an overview on the wind direction over the glacier, and does not give information on the kind of forcing leading to the wind direction shift. Whiteman and Doran (1993) defined four scenarios of interactions between the (synoptic) flow aloft and the flow within a valley: thermally-driven, downward momentum transport by gravity waves, forced channeling, and pressure-driven channelling. To learn about which forcing is responsible for the wind direction in the glacier valley in our simulations, the wind direction of the synoptic flow aloft (in our case the upstream location) and the wind direction of the valley flow can be compared. The resulting pattern (Fig. 6b) shows whether the flow falls into one of the four categories of Whiteman and Doran (1993). In the REF simulation, the points collapse onto a diagonal line, suggesting that the wind structure in the HEF valley is indeed dominated by downward momentum transport by the gravity wave. For the NO_GL and NO_UP simulations, a different picture emerges: Some of the points still follow the diagonal line (hence, downward momentum transport), but most of the points are either present in the lower left or lower right corner. This pattern corresponds to forced channelling, where the synoptic flow is channelled into the valley. In theory, pressure-driven channeling could also be a reason for the up-glacier flow (with a slightly different wind direction pattern), but this requires a horizontal pressure gradient along the valley axis. We calculated the horizontal pressure gradient (not shown), but it showed no distinct signal, hence we conclude that forced channelling is the major mechanism at play in the simulations without the upstream glaciers. In general, shallow valleys (e.g., the Rhine Valley or the Tennessee Valley) are more prone to channelling of synoptic flows (Whiteman and Doran, 1993; Steyn et al., 2013) than deep Alpine valleys like the Inn Valley, where thermally-induced flows are very resilient to synoptic influence (Zängl, 2009). Given that the HEF valley is also rather shallow compared to its surroundings (the height difference between HEF tongue and the upstream location is around 500 m), channelling of synoptic cross-glacier flows is a realistic scenario. To summarize, we conclude that the gravity wave leads to downward momentum transport over the HEF valley, and when it breaks and henceforth weakens, the synoptic flow is channelled via forced channelling into the glacier valley. In this case study, the up-glacier flows after 09:00 UTC can be explained with dynamical forcing and and the thermal forcing component (e.g., slope/valley flow due to differential heating) is negligible.

https://doi.org/10.5194/egusphere-2024-2634
Preprint. Discussion started: 27 August 2024

4 Impact on glacier boundary layer

We described the major features of the wind patterns and gravity wave formation in the NO_UP and NO_GL simulations in compared to the REF simulation in the previous Sections. In this Section, we will compare the three simulations with respect to sensible heat fluxes, advection patterns, and 2 m temperature.

The energy exchange over mountain glaciers is - especially during the summer months - strongly influenced by the sensible heat flux at the glacier surface. In the typical application of bulk formulation of turbulent fluxes to glacier surfaces, sensible heat fluxes over glaciers strongly depend on the wind speed, and to some extent also on the wind direction, dependent on whether the flow origin is, e.g., up-glacier (which would suggest a katabatic glacier wind is present and henceforth cool advection), or cross- or up-glacier (with warm advection) under clear-sky conditions.

4.1 Spatial patterns of sensible heat flux

In the REF simulation with the realistic glacier surfaces, we note that the sensible heat flux is negative (from the ice to the atmosphere, atmospheric notation) during the entire simulation time (Fig. 7a,d,g,j). Over the remaining ice surface (i.e., HEF) in NO_UP, sensible heat fluxes are already reduced by 50 W m^{-2} compared to REF at 06:00 UTC (Fig. 7b). This patterns continues during the entire simulation time at the remaining ice surface in NO_UP. Interestingly, the sensible heat flux difference between NO_UP and REF is very small at the upper part of the remaining glacier, where cross-glacier flow is present (Fig. 7h,k,i,l). The largest differences between REF and NO_UP are visible at 12:00 UTC, when the gravity wave broke and the strong up-glacier flow is present (Fig. 7i,l). It is not surprising the sensible heat fluxes over the missing ice surfaces change sign and are positive now which range up to 500 W m^{-2} between REF and NO_UP (Fig. 7k). Still, even on the slope between the (missing glaciers) and HEF sensible heat fluxes are now higher in the NO_UP simulation, which is likely related to the strong turbulent mixing induced by the earlier breaking gravity wave in NO_UP and advection processes (see next section). This indicated that the missing upstream glaciers with their influence on atmospheric flow structure and the resulting spatial variability in sensible heat fluxes have a potential impact on HEF's melting patterns.

When we remove all glaciers from the model domain (Fig. 8), sensible heat fluxes reveal a large difference between NO_GL and REF changing over simulation time. At 06:00 UTC, SH fluxes exhibit a difference of around 100 W m^{-2} over the missing ice surfaces (Fig. 8b), while with progressing simulation time these differences change up to more than 500 W m^{-2} with opposite signs (Fig. 8k). This is not surprising, since changing the land-use category in the model from "ice" to "bare rock" leads to changes in albedo and roughness length, henceforth leading to positive sensible heat fluxes during the daytime. Interestingly, sensible heat fluxes remain smaller in the glacier valley than its surroundings in the NO_GL simulation (Fig. 8c,f,i,l), likely due to the sheltered location of the valley and topographic shading. Highest sensible heat flux values are recognizable at the mountain ridges and in regions with high wind speeds.

https://doi.org/10.5194/egusphere-2024-2634
Preprint. Discussion started: 27 August 2024

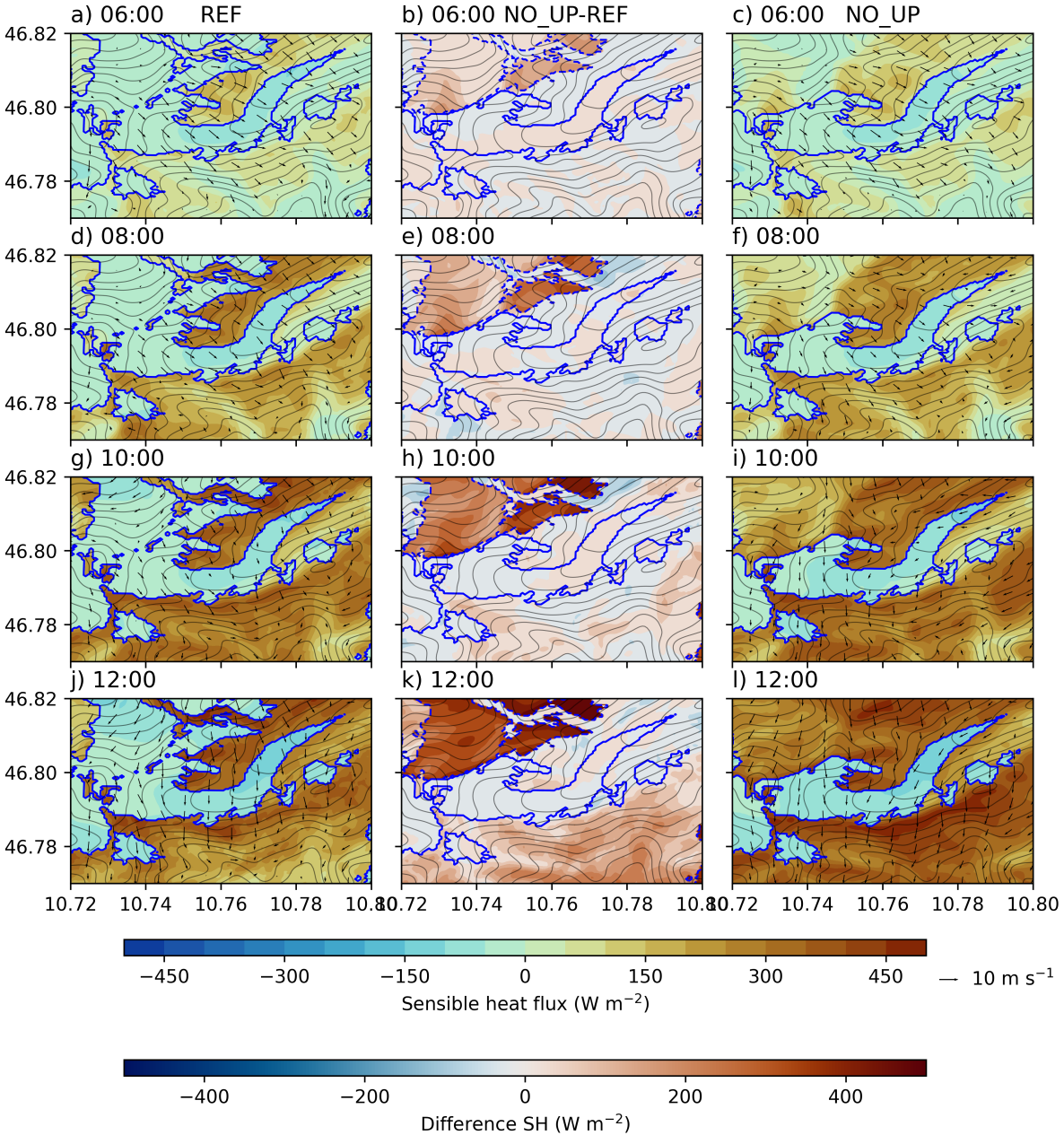

Figure 7. Simulated sensible heat flux (colors) from the lowest model level at four different times (06:00 UTC, a-c; 08:00 UTC, d-e; 10:00 UTC, g-i; 12:00 UTC, j-i). Left row: REF; middle: Difference between REF and NO_UP, right row: NO_UP. The blue contours represent the glacier outlines in the simulations, while dashed blue lines in the middle row indicate the 'missing' ice surfaces. The thin black contours show model topography.

https://doi.org/10.5194/egusphere-2024-2634
Preprint. Discussion started: 27 August 2024

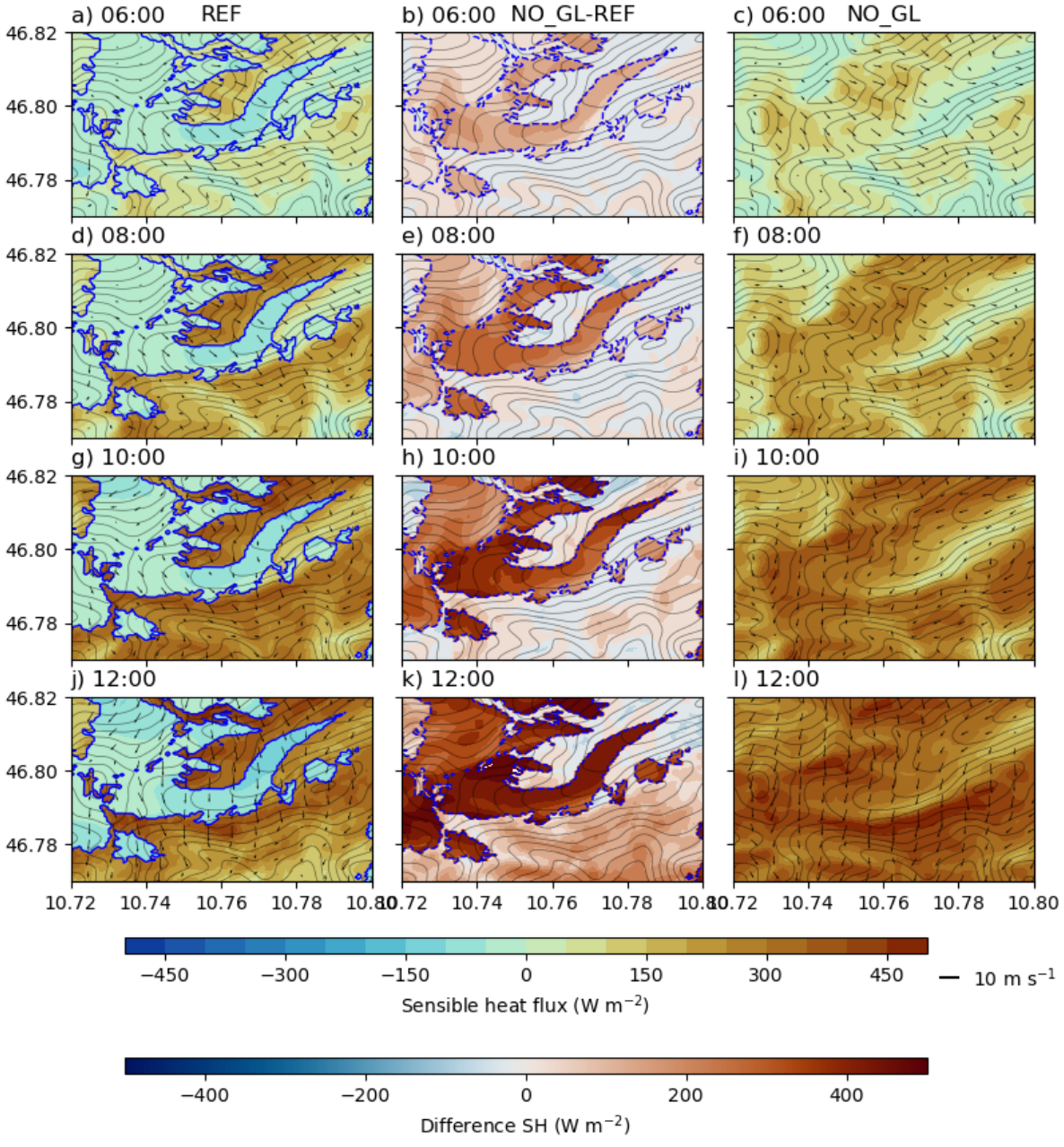

Figure 8. Simulated Sensible heat flux (colors) from the lowest model level and 10 m wind speed (black arrows) at four different times (06:00 UTC, a-c; 08:00 UTC, d-e; 10:00 UTC, g-i; 12:00 UTC, j-i). Left row: REF; middle: Difference between REF and NO_GL, right row: NO_GL. The blue contours represent the glacier outlines in the simulations, while dashed blue lines indicate the 'missing' ice surfaces. The thin black contours show model topography.

https://doi.org/10.5194/egusphere-2024-2634
Preprint. Discussion started: 27 August 2024

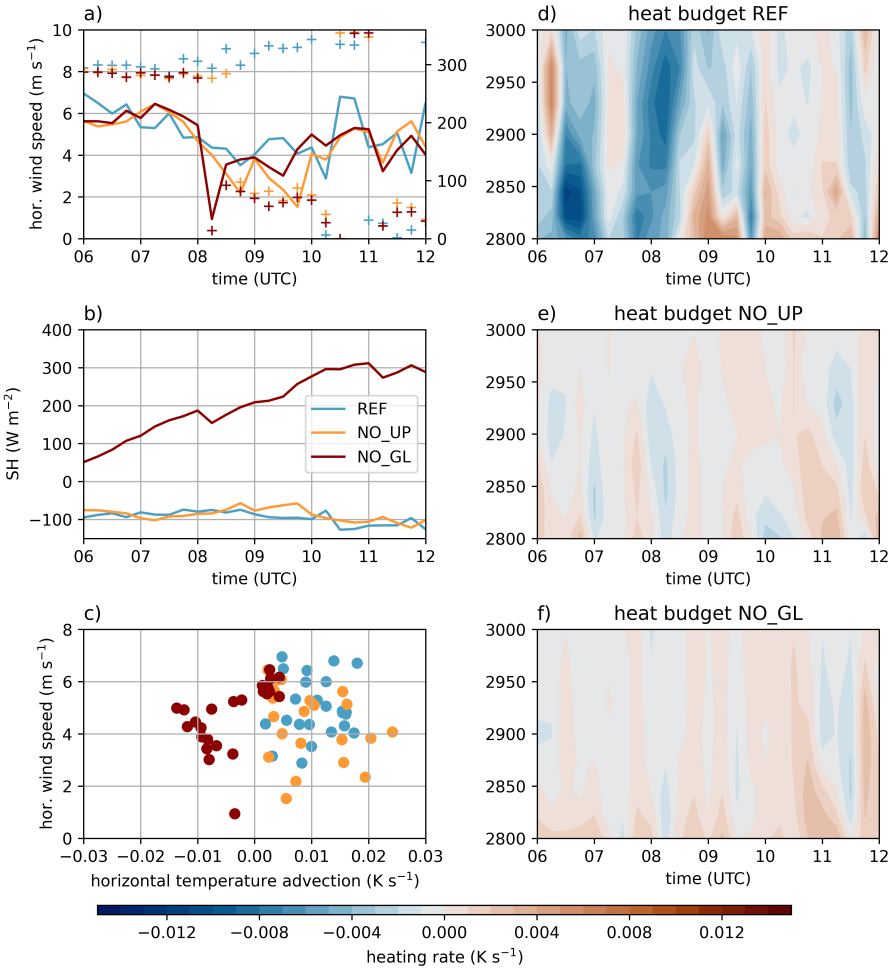

Figure 9. Panel a) Time series of horizontal wind speed (lines) and wind direction (+) for REF (blue), NO_UP (orange), and NO_GL (red) simulations at HEF tongue. Panel b) as panel a), but for sensible heat flux. Panel c) Scatter plot of horizontal temperature advection and horizontal wind speed over the time period of interest. Panels d)-f) Time series of the total heat budget over HEF tongue for REF (d), NO_UP (e), and NO_GL (f) simulations.

4.2 Advection patterns

Time series of horizontal wind speed and direction at HEF tongue (Fig. 9a) reveal no large differences in the absolute values of wind speeds between REF, NO_UP, and NO_GL. However, there is a clear difference in wind direction, where the up-glacier flow develops after 08:00 UTC related to the earlier gravity wave breaking in the NO_UP simulation. Time series of sensible heat flux at HEF tongue (Fig. 7) suggest weaker sensible heat fluxes in the NO_UP simulation compared to REF (Fig. 9b), while sensible heat fluxes in the NO_GL simulation are entirely positive. The glacier tongue is in REF and NO_UP simulations during the entire time period of interest under the influence of horizontal warm-air advection (Fig. 9c). While this is mostly

https://doi.org/10.5194/egusphere-2024-2634
Preprint. Discussion started: 27 August 2024

associated with the gravity wave and cross-glacier flow in the REF simulation, also up-glacier flow leads to stronger warm-air advection over HEF tongue. In theory, we could have assumed that the cross-glacier flow enhances the katabatic glacier wind from the upstream glaciers and would lead to cold-air advection of HEF tongue, however, this did prove as not true given that the horizontal warm-air advection patterns are very similar in the REF and NO_UP simulations (Fig. 9c). In the NO_GL simulation, the location of the missing glacier is under the influence of cold-air advection, which is surprising at the first glance. However, the surface is not cooler than its environment anymore due to the entirely missing ice surfaces, and it is likely that colder air is advected by the gravity wave from aloft.

When we consider the total vertical heat budget, we calculate it as in Goger et al. (2022):

$$\frac{\partial \theta}{\partial t} = \underbrace{-U\frac{\partial \theta}{\partial x} - V\frac{\partial \theta}{\partial y} - W\frac{\partial \theta}{\partial z}}_{Adv} - \underbrace{\frac{\partial \overline{w'\theta'}}{\partial z}}_{vHFD} \tag{3}$$

with temperature advection with the mean wind in all three directions (ADV) and the vertical heat flux divergence (vHFD). The heat budget of the REF simulation (Fig. 9d) reveals cooling of the column above HEF tongue between 06:00 and 08:30 UTC, with slight interruptions above 2800 m a.g. with a wavy structure. This is likely related to the gravity wave pattern, and since it does not break before 08:30, the glacier remains under cold-air advection. This pattern changes with the gravity wave breaking, the glacier is suddenly under warming until 12:00 UTC. In the NO_UP simulation, a different picture emerges (Fig. 9e) : HEF tongue is under influence of either cooling or heating, but not as continuous as in REF and also with weaker absolute heating values. Similar patterns are visible in the NO_GL simulation (Fig. 9f) with stronger warming effects. We relate this phenomenon to the much weaker gravity wave (which breaks earlier) in the simulation without the upstream glaciers, which has a large influence on the heating rate over the glacier. To summarize, when we consider the vertical heating rate, large differences are present between the two simulations; while REF shows distinct heating or cooling patterns in relation to the gravity wave, the patterns in the NO_UP and NO_GL simulations show a general warming effect.

4.3 Resulting temperature structure on the glacier

Finally, the impact of changing the glacier surfaces on the 2 m temperature is shown in Figure 10. We choose the (diagnostic) 2 m temperature instead of the skin temperature, because the skin temperature is constant at 0°C over the melting glacier, but the 2 m temperature is closest to the surface and gives an overview of near-surface thermal conditions, athough we have to keep in mind that the formulae calculating 2 m temperature still rely on Monin-Obukhov similarity theory (Monin and Obukhov, 1954; Jiménez et al., 2012). The 2 m temperature, averaged over our time period of interest (06:00–12:00 UTC) shows temperatures close to zero over all ice surfaces, especially over the upstream glaciers (Fig. 10a), while the glacier surroundings are up to 10°C warmer. The NO_UP simulation shows higher 2 m temperatures over the missing upstream glaciers with a temperature contrast of up to 5°C compared to REF (Fig. 10b). Furthermore, HEF tongue is warmer by 1°C than the REF counterpart (Fig. 10c), suggesting that the glacier tongue is influenced by the (warmer) surroundings, due to warm air advection (cf. Fig. 9. Finally, removing all glaciers (Fig. 10c) leads to a temperature increase of 5°C at all missing ice surfaces compared to REF.

https://doi.org/10.5194/egusphere-2024-2634
Preprint. Discussion started: 27 August 2024

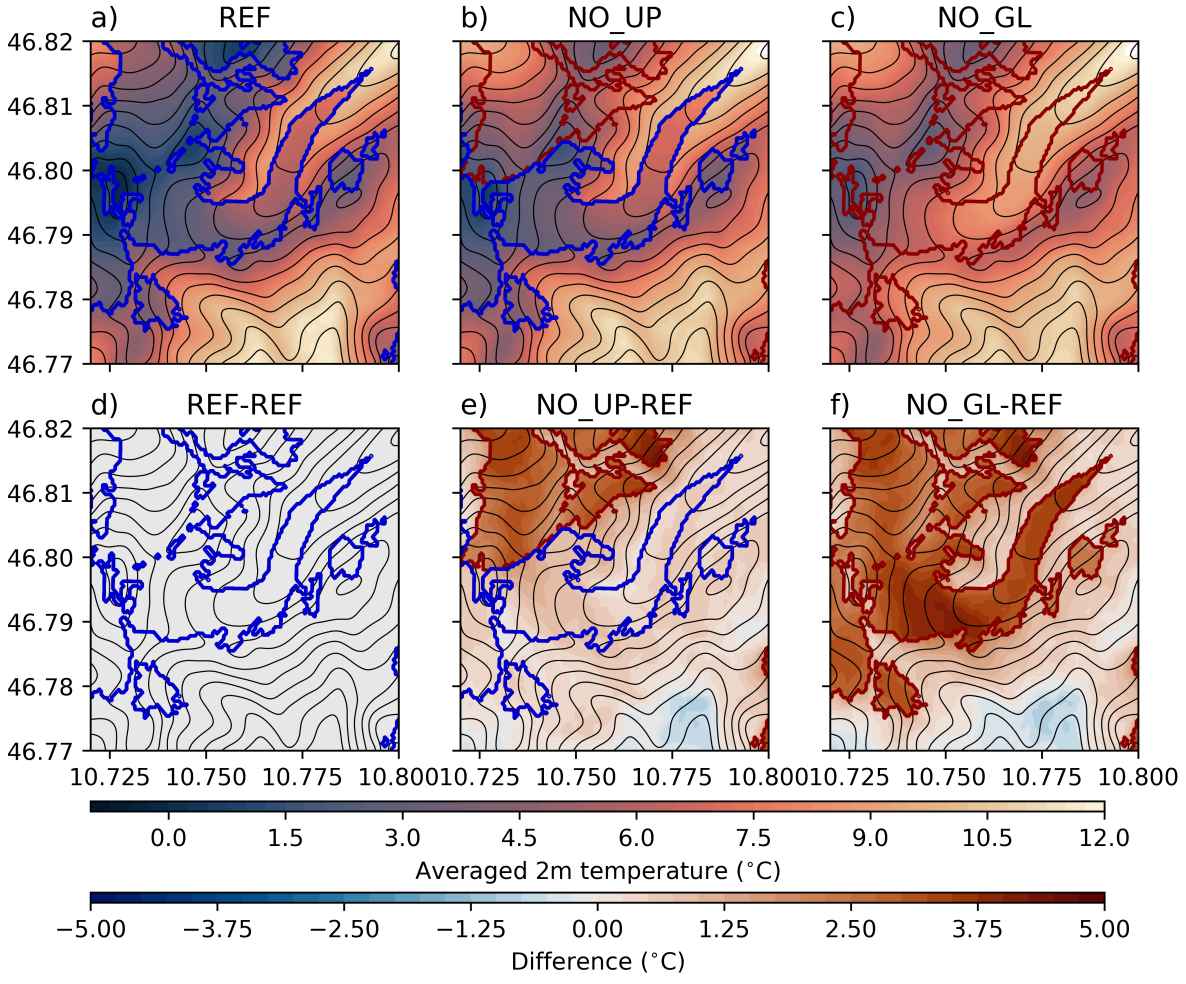

Figure 10. Panels a-c) Averaged 2 m temperature (colors) over the simulation period of interest (06:00–12 UTC) for REF, NO_UP, and NO_GL, respectively. Panels d-f) Difference in averaged 2 m temperature from REF. All panels: Topography (black contours), ice surfaces (blue outlines), missing ice surfaces compared to REF (red outlines).

The surroundings also are by 1°C warmer than REF (Fig. 10f), suggesting a strong influence by the strong turbulent mixing induced by the breaking gravity wave.

5 Discussion

In general, our LES simulations proved as an ideal test bed to study the impact of dynamically-induced flows on the glacier boundary layer. As already discussed in Goger et al. (2022) and Voordendag et al. (2024), we have to note that despite our high horizontal and vertical resolution ($\Delta x = 48$ m and lowest model half-level at $z = 3$ m), we cannot assume that the local glacier

https://doi.org/10.5194/egusphere-2024-2634
Preprint. Discussion started: 27 August 2024

boundary layer with the katabatic down-glacier wind is simulated realistically. Observations by Mott et al. (2020) over HEF suggest that the katabatic jet is located at 2 m above the ice surface. Given that, strictly speaking, a LES of stable boundary layer would require $\Delta x = 1$ m according to Cuxart (2015), which is currently not possible with the WRF model. Still, more than 10 grid points across the glacier valley are present in our domain, and this hints that the major ABL processes are resolved (Wagner et al., 2014). In this study, however, we focus on dynamical aspects and gravity waves, which form on scales larger than the small-scale glacier boundary layer, and therefore we can expect that the model delivers reliable results on these processes.

We mostly analyzed results from 6 hours of simulation time (06:00-12:00 UTC), not only because REF started to deviate from observations after 12:00 UTC (Goger et al., 2022), but also, because the two sensitivity simulations (NO_UP and NO_GL) did not give new insights on the gravity wave dynamics: In both NO_UP and NO_GL, the gravity wave does not re-establish itself and up-glacier flow prevails as in the REF simulation after 12:00 UTC (not shown). Although the simulations are semi-idealized, results suggest that HEF cannot be seen as an individual isolated glacier in terms of its boundary-layer development. While we only show findings from a single case study, it is clear that HEF is strongly affected by the upstream glaciers under North-Westerly flow, given their strong influence on gravity wave formation. The gravity wave is most persistent in the REF simulation, not only because of the stronger stability over the upstream glaciers, but also because cold air is present above HEF hindering an immediate plunge into the glacier valley. A study of foehn flows over the Larsen C ice shelf, Antartica by Turton et al. (2018) found that the stabilizing effect of upstream ice surfaces indeed influences the isentrope drawdown of gravity waves. Jonassen et al. (2014) simulated gravity waves over the Hofsjökull icecap, Iceland, and also found stronger downslope flow acceleration in simulations with the icecap, while removing the icecap from the domain led to weaker downslope flows.

Although our study is located in a different region and especially at smaller scales, we found an agreement with the aforementioned literature. A gravity wave is present in both the NO_UP and NO_GL simulations, but it is weaker and breaks earlier, leading to strong turbulent mixing and an earlier. The force balance due to gravity wave breaking changes the flow regime inside the valley from across glacier caused by downward momentum transport, to up-valley due to forced channeling. This up-valley flow might be additionally supported by thermally driven up-valley flows, but is primarily of dynamic nature. Due to the gravity wave breaking, the synoptic flow is channelled into the glacier valley, resulting in a change of wind direction towards up-glacier, ultimately affecting sensible heat fluxes and advection patterns. Another interesting aspect is that the flow structure in the NO_UP and NO_GL simulations are very similar, despite the presence of the glacier tongue in the NO_UP simulation. This suggests that in our particular case study the flow structure in the glacier valley is so strongly dominated by the upstream conditions, so that local effects by HEF itself do not have a large impact on local wind patterns. The upstream glaciers play a relevant role in influencing the upstream flow structure, and henceforth the local flows over HEF. Given that, it makes sense to speak of a *system* of glaciers influencing each other's local micro-climates on a scale of around 5 km - similar as in Conway et al. (2021) speaking about ice field breezes instead of looking at isolated glacier tongues.

https://doi.org/10.5194/egusphere-2024-2634
Preprint. Discussion started: 27 August 2024

6 Conclusions

We conducted semi-idealized large-eddy simulations at Δx =48 m over the Hinterisferner (HEF) glacier in the Austrian Alps of a case study with North-Westerly synoptic flow. The reference simulation (REF) was run with realistic glacier surfaces, while the NO_UP simulation ran without upstream glaciers, and in the NO_GL simulation all ice surfaces were removed from the domain. The results allow us to draw the following conclusions:

- Under North-Westerly synoptic flow, a gravity wave forms over HEF's tongue in all three simulations, which eventually breaks leading to turbulent mixing over the glacier surface.
- Removing the upstream glaciers in the NO_UP simulation leads to a neutral stratification with an unstable surface layer and henceforth less favorable conditions for gravity wave formation. The gravity wave in the NO_UP simulation is weaker than in REF and breaks earlier, leading to strong turbulent mixing over the remaining glacier surface and finally changing the cross-glacier flow towards up-glacier. A similar pattern is present in the NO_GL simulation.
- The upstream glaciers are not *necessary* for gravity wave formation, but *strongly* influence their strength by stabilizing the upstream profile.
- The wind patterns in the glacier valley are governed by downward momentum transport by the gravity wave. When it breaks, the synoptic flow is channelled into the valley leading to up-glacier flows.
- Due to the changed gravity wave structure, higher temperatures, a higher spatial variability in sensible heat fluxes, and a overall positive heat budget are present at HEF tongue in the NO_UP and NO_GL simulations.
- The local boundary layer in the NO_GL simulation is very similar to the NO_UP simulation, suggesting that the local glacier boundary layer over HEF is therefore less governed by the surface below (ice), and rather by dynamical forcing.
- The results suggest that HEF is not isolated from its nearby environment (rock surface/slopes), and that the influence of upstream ice surfaces on local ABL development cannot be disregarded. Henceforth, it makes sense to investigate a *system* of glaciers instead of only studying processes on isolated glacier tongues in the near future.

The present study gave insight to the impact of ice surfaces on gravity wave formation and breaking affecting glacier boundary layer development. In the future, similar studies with different upstream conditions could be conducted. However, one of the open questions in glacier boundary layer dynamics is still the future changes in glacier boundary-layer structure in a warming climate, which could be quantified with high-resolution LES using ice surfaces from future climate projections.

Code and data availability. The WRF v4.1 model code can be downloaded from github (WRF, 2019), and the averaging module "WRF LES diagnostics" is available at Umek (2020). The model output is available upon request from BG. Figures were generated with python-matplotlib (Hunter, 2007) using colormaps by Crameri (2023).

https://doi.org/10.5194/egusphere-2024-2634
Preprint. Discussion started: 27 August 2024

Author contributions. BG set up and conducted the numerical simulations and wrote the initial draft of the manuscript. MO conducted the analysis of numerical data within his internship at Universität Innsbruck in summer 2023. IS had the idea of modifying glacier surfaces for an additional study on glacier boundary layer dynamics, and LN provided input from a glaciologist's perspective. All authors read and improved the manuscript where necessary.

Competing interests. The authors declare no competing interests.

Acknowledgements. This work is part of the project "Measuring and modeling snow-cover dynamics at high resolution for improving distributed mass balance research on mountain glaciers", a joint project fully funded by the Austrian Science Foundation (FWF, project number I 3841-N32, https://dx.doi.org/10.55776/I3841) and the Deutsche Forschungsgemeinschaft (DFG; project number SA 2339/7-1). The computational results presented have been achieved using the Vienna Scientific Cluster (VSC) under project number 71434. The work of I. Stiperski was funded through the European Research Council (ERC) under the European Union's Horizon 2020 research and innovation program (Grant agreement No. 101001691).

https://doi.org/10.5194/egusphere-2024-2634
Preprint. Discussion started: 27 August 2024

References

WRF Version 4.1, https://github.com/wrf-model/WRF/releases/tag/v4.1, 2019.

Beniston, M., Farinotti, D., Stoffel, M., Andreassen, L. M., Coppola, E., Eckert, N., Fantini, A., Giacona, F., Hauck, C., Huss, M., Huwald, H., Lehning, M., López-Moreno, J.-I., Magnusson, J., Marty, C., Morán-Tejéda, E., Morin, S., Naaim, M., Provenzale, A., Rabatel, A., Six, D., Stötter, J., Strasser, U., Terzago, S., and Vincent, C.: The European mountain cryosphere: a review of its current state, trends, and future challenges, The Cryosphere, 12, 759–794, https://doi.org/10.5194/tc-12-759-2018, 2018.

Byrne, M. P., Boos, W. R., and Hu, S.: Elevation-dependent warming: observations, models, and energetic mechanisms, Weather Clim Dyn, 5, 763–777, https://doi.org/10.5194/wcd-5-763-2024, 2024.

Conway, J. P., Helgason, W. D., Pomeroy, J. W., and Sicart, J. E.: Icefield Breezes: Mesoscale Diurnal Circulation in the Atmospheric Boundary Layer Over an Outlet of the Columbia Icefield, Canadian Rockies, J. Geophys. Res. Atmos., 126, e2020JD034 225, https://doi.org/10.1029/2020JD034225, 2021.

Crameri, F.: Scientific colour maps, https://doi.org/10.5281/zenodo.8035877, 2023.

Cremona, A., Huss, M., Landmann, J. M., Borner, J., and Farinotti, D.: European heat waves 2022: contribution to extreme glacier melt in Switzerland inferred from automated ablation readings, The Cryosphere, 17, 1895–1912, https://doi.org/10.5194/tc-17-1895-2023, 2023.

Cuxart, J.: When Can a High-Resolution Simulation Over Complex Terrain be Called LES?, Front. Earth Sci., 3, 6, https://doi.org/10.3389/feart.2015.00087, 2015.

Deardorff, J. W.: Stratocumulus-capped mixed layers derived from a three-dimensional model, Boundary-Layer Meteorol., 18, 495–527, https://doi.org/10.1007/BF00119502, 1980.

Draeger, C., Radić, V., White, R. H., and Tessema, M. A.: Evaluation of reanalysis data and dynamical downscaling for surface energy balance modeling at mountain glaciers in western Canada, The Cryosphere, 18, 17–42, https://doi.org/10.5194/tc-18-17-2024, 2024.

Egger, J. and Kühnel, R.: Orographic gravity waves induced by variable mean winds: observations at Hofsjokull, Meteorol. Z., 19, 101–113, https://doi.org/10.1127/0941-2948/2010/0427, 2010.

Finnigan, J. J. and Einaudi, F.: The interaction between an internal gravity wave and the planetary boundary layer. Part II: Effect of the wave on the turbulence structure, Q. J. R. Meteorol. Soc., 107, 807–832, https://doi.org/10.1002/qj.49710745405, 1981.

Gerber, F., Besic, N., Sharma, V., Mott, R., Daniels, M., Gabella, M., Berne, A., Germann, U., and Lehning, M.: Spatial variability in snow precipitation and accumulation in COSMO–WRF simulations and radar estimations over complex terrain, The Cryosphere, 12, 3137–3160, https://doi.org/10.5194/tc-12-3137-2018, 2018.

Goger, B. and Dipankar, A.: The impact of mesh size, turbulence parameterization, and land-surface-exchange scheme on simulations of the mountain boundary layer in the hectometric range, Q. J. R. Meteorol. Soc., https://doi.org/10.1002/qj.4799, 2024.

Goger, B., Stiperski, I., Nicholson, L., and Sauter, T.: Large-eddy simulations of the atmospheric boundary layer over an Alpine glacier: Impact of synoptic flow direction and governing processes, Q. J. R. Meteorol. Soc, 148, 1319–1343, https://doi.org/10.1002/qj.4263, 2022.

Haid, M., Gohm, A., Umek, L., Ward, H. C., and Rotach, M. W.: Cold-Air Pool Processes in the Inn Valley During Föhn: A Comparison of Four Cases During the PIANO Campaign, Boundary-Layer Meteorol., 182, 335–362, https://doi.org/10.1007/s10546-021-00663-9, 2022.

Heinze, R., Dipankar, A., Carbajal Henken, C., Moseley, C., Sourdeval, O., Trömel, S., Xie, X., Adamidis, P., Ament, F., Baars, H., Barthlott, C., Behrendt, A., Blahak, U., Bley, S., Brdar, S., Brueck, M., Crewell, S., Deneke, H., Di Girolamo, P., Evaristo, R., Fischer, J., Frank, C., Friederichs, P., Göcke, T., Gorges, K., Hande, L., Hanke, M., Hansen, A., Hege, H.-C., Hoose, C., Jahns, T., Kalthoff, N., Klocke,

https://doi.org/10.5194/egusphere-2024-2634
Preprint. Discussion started: 27 August 2024

D., Kneifel, S., Knippertz, P., Kuhn, A., van Laar, T., Macke, A., Maurer, V., Mayer, B., Meyer, C. I., Muppa, S. K., Neggers, R. A. J., Orlandi, E., Pantillon, F., Pospichal, B., Röber, N., Scheck, L., Seifert, A., Seifert, P., Senf, F., Siligam, P., Simmer, C., Steinke, S., Stevens, B., Wapler, K., Weniger, M., Wulfmeyer, V., Zängl, G., Zhang, D., and Quaas, J.: Large-eddy simulations over Germany using ICON: A comprehensive evaluation, Q. J. R. Meteorol. Soc., 143, 69–100, https://doi.org/10.1002/qj.2947, 2017.

Hersbach, H., Bell, B., Berrisford, P., Hirahara, S., Horányi, A., Muñoz Sabater, J., Nicolas, J., Peubey, C., Radu, R., Schepers, D., Simmons, A., Soci, C., Abdalla, S., Abellan, X., Balsamo, G., Bechtold, P., Biavati, G., Bidlot, J., Bonavita, M., De Chiara, G., Dahlgren, P., Dee, D., Diamantakis, M., Dragani, R., Flemming, J., Forbes, R., Fuentes, M., Geer, A., Haimberger, L., Healy, S., Hogan, R. J., Hólm, E., Janisková, M., Keeley, S., Laloyaux, P., Lopez, P., Lupu, C., Radnoti, G., de Rosnay, P., Rozum, I., Vamborg, F., Villaume, S., and Thépaut, J.-N.: The ERA5 global reanalysis, Q. J. R. Meteorol. Soc., 146, 1999–2049, https://doi.org/10.1002/qj.3803, 2020.

Hock, R., Rasul, G., Adler, C., Cáceres, B., Gruber, S., Hirabayashi, Y., Jackson, M., Kääb, A., Kang, S., Kutuzov, S., Milner, A., Molau, U., Morin, S., Orlove, B., and Steltzer, H.: High Mountain Areas, in: IPCC Special Report on the Ocean and Cryosphere in a Changing Climate, edited by Pörtner, H.-O., Roberts, D., Masson-Delmotte, V., Zhai, P., Tignor, M., Poloczanska, E., Mintenbeck, K., Alegría, A., Nicolai, M., Okem, A., Petzold, J., Rama, B., and Weyer, N., pp. 131–202, Cambridge University Press, https://doi.org/10.1017/9781009157964.004, 2022.

Hunter, J. D.: Matplotlib: A 2D Graphics Environment, Comput. Sci. & Eng., 9, 90–95, https://doi.org/10.1109/MCSE.2007.55, 2007.

Iacono, M. J., Delamere, J. S., Mlawer, E. J., Shephard, M. W., Clough, S. A., and Collins, W. D.: Radiative forcing by long-lived greenhouse gases: Calculations with the AER radiative transfer models, J. Geophys. Res. Atmos., 113, https://doi.org/10.1029/2008JD009944, 2008.

Jackson, P. L., Mayr, G., and Vosper, S.: Dynamically-Driven Winds, in: Mountain Weather Research and Forecasting, edited by Chow, F. K., De Wekker, S. F. J., and Snyder, B. J., Springer Atmospheric Sciences, pp. 121–218, Springer Netherlands, https://doi.org/10.1007/978-94-007-4098-3_3, 2013.

Jiang, Q. and Doyle, J. D.: Gravity Wave Breaking over the Central Alps: Role of Complex Terrain, J. Atmos. Sci., 61, 2249 – 2266, https://doi.org/10.1175/1520-0469(2004)061<2249:GWBOTC>2.0.CO;2, 2004.

Jiménez, P. A., Dudhia, J., González-Rouco, J. F., Navarro, J., Montávez, J. P., and García-Bustamante, E.: A Revised Scheme for the WRF Surface Layer Formulation, Mon. Wea. Rev., 140, 898 – 918, https://doi.org/10.1175/MWR-D-11-00056.1, 2012.

Jonassen, M. O., Ágústsson, H., and Ólafsson, H.: Impact of surface characteristics on flow over a mesoscale mountain, Q. J. R. Meteorol. Soc., 140, 2330–2341, https://doi.org/10.1002/qj.2302, 2014.

Kiszler, T., Ebell, K., and Schemann, V.: A Performance Baseline for the Representation of Clouds and Humidity in Cloud-Resolving ICON-LEM Simulations in the Arctic, J Adv Model Earth Sys, 15, e2022MS003 299, https://doi.org/10.1029/2022MS003299, e2022MS003299 2022MS003299, 2023.

Lehner, M.: The Boundary Layer Over Complex Terrain, in: Reference Module in Earth Systems and Environmental Sciences, Elsevier, https://doi.org/10.1016/B978-0-323-96026-7.00075-8, 2024.

Litt, M., Sicart, J.-E., Six, D., Wagnon, P., and Helgason, W. D.: Surface-layer turbulence, energy balance and links to atmospheric circulations over a mountain glacier in the French Alps, The Cryosphere, 11, 971–987, https://doi.org/10.5194/tc-11-971-2017, 2017.

Lott, F.: A New Theory for Downslope Windstorms and Trapped Mountain Waves, J. Atmos. Sci., 73, 3585 – 3597, https://doi.org/10.1175/JAS-D-15-0342.1, 2016.

Matiu, M., Crespi, A., Bertoldi, G., Carmagnola, C. M., Marty, C., Morin, S., Schöner, W., Cat Berro, D., Chiogna, G., De Gregorio, L., Kotlarski, S., Majone, B., Resch, G., Terzago, S., Valt, M., Beozzo, W., Cianfarra, P., Gouttevin, I., Marcolini, G., Notarnicola, C., Petitta, M., Scherrer, S. C., Strasser, U., Winkler, M., Zebisch, M., Cicogna, A., Cremonini, R., Debernardi, A., Faletto, M., Gaddo, M.,

https://doi.org/10.5194/egusphere-2024-2634
Preprint. Discussion started: 27 August 2024

Giovannini, L., Mercalli, L., Soubeyroux, J.-M., Sušnik, A., Trenti, A., Urbani, S., and Weilguni, V.: Observed snow depth trends in the European Alps: 1971 to 2019, The Cryosphere, 15, 1343–1382, https://doi.org/10.5194/tc-15-1343-2021, 2021.

Monin, A. S. and Obukhov, A. M.: Osnovnye zakonomernosti turbulentnogo peremeshivanija v prizemnom sloe atmosfery (Basic Laws of Turbulent Mixing in the Atmosphere Near the Ground), Trudy geofiz. inst. AN SSSR, 24, 163–187, 1954.

Mott, R., Stiperski, I., and Nicholson, L.: Spatio-temporal flow variations driving heat exchange processes at a mountain glacier, The Cryosphere, 14, 4699–4718, https://doi.org/10.5194/tc-14-4699-2020, 2020.

Nicholson, L. and Stiperski, I.: Comparison of turbulent structures and energy fluxes over exposed and debris-covered glacier ice, J. Glaciol., pp. 1–13, https://doi.org/10.1017/jog.2020.23, 2020.

Obleitner, F.: Climatological features of glacier and valley winds at the Hintereisferner (Ötztal Alps, Austria), Theor. Appl. Climatol., 49, 225–239, https://doi.org/10.1007/BF00867462, 1994.

Oerlemans, J. F.: The microclimate of valley glaciers, IGITUR, Universiteitsbibliotheek Utrecht, https://dspace.library.uu.nl/handle/1874/202997, 2010.

Omanovic, N., Goger, B., and Lohmann, U.: The impact of mesh size and microphysics scheme on the representation of mid-level clouds in the ICON model in hilly and complex terrain, EGUsphere, 2024, 1–43, https://doi.org/10.5194/egusphere-2024-1989, 2024.

Parmhed, O., Oerlemans, J., and Grisogono, B.: Describing surface fluxes in katabatic flow on Breidamerkurjökull, Iceland, Q. J. R. Meteorol. Soc., 130, 1137–1151, https://doi.org/10.1256/qj.03.52, 2004.

Piermattei, L., Zemp, M., Sommer, C., Brun, F., Braun, M. H., Andreassen, L. M., Belart, J. M. C., Berthier, E., Bhattacharya, A., Boehm Vock, L., Bolch, T., Dehecq, A., Dussaillant, I., Falaschi, D., Florentine, C., Floricioiu, D., Ginzler, C., Guillet, G., Hugonnet, R., Huss, M., Kääb, A., King, O., Klug, C., Knuth, F., Krieger, L., La Frenierre, J., McNabb, R., McNeil, C., Prinz, R., Sass, L., Seehaus, T., Shean, D., Treichler, D., Wendt, A., and Yang, R.: Observing glacier elevation changes from spaceborne optical and radar sensors – an inter-comparison experiment using ASTER and TanDEM-X data, The Cryosphere, 18, 3195–3230, https://doi.org/10.5194/tc-18-3195-2024, 2024.

Reuder, J., Ablinger, M., Ágústsson, H., Brisset, P., Brynjólfsson, S., Garhammer, M., Jóhannesson, T., Jonassen, M. O., Kühnel, R., Lämmlein, S., de Lange, T., Lindenberg, C., Malardel, S., Mayer, S., Müller, M., Ólafsson, H., Rögnvaldsson, Ó., Schäper, W., Spengler, T., Zängl, G., and Egger, J.: FLOHOF 2007: an overview of the mesoscale meteorological field campaign at Hofsjökull, Central Iceland, Meteorol. Atmos. Phys., 116, 1–13, https://doi.org/10.1007/s00703-010-0118-4, 2012.

Rotach, M. W. and Zardi, D.: On the boundary-layer structure over highly complex terrain: Key findings from MAP, Q. J. R. Meteorol. Soc., 133, 937–948, https://doi.org/10.1002/qj.71, 2007.

Sauter, T. and Galos, S. P.: Effects of local advection on the spatial sensible heat flux variation on a mountain glacier, The Cryosphere, 10, 2887–2905, https://doi.org/10.5194/tc-10-2887-2016, 2016.

Scorer, R. S.: Theory of waves in the lee of mountains, Q. J. R. Meteorol. Soc., 75, 41–56, https://doi.org/10.1002/qj.49707532308, 1949.

Shaw, T. E., Buri, P., McCarthy, M., Miles, E. S., Ayala, A., and Pellicciotti, F.: The Decaying Near-Surface Boundary Layer of a Retreating Alpine Glacier, Geophys Res Lett, 50, e2023GL103 043, https://doi.org/10.1029/2023GL103043, 2023.

Shaw, T. E., Buri, P., McCarthy, M., Miles, E. S., and Pellicciotti, F.: Local Controls on Near-Surface Glacier Cooling Under Warm Atmospheric Conditions, J Geophys Res. Atmospheres, 129, e2023JD040 214, https://doi.org/10.1029/2023JD040214, e2023JD040214 2023JD040214, 2024.

https://doi.org/10.5194/egusphere-2024-2634
Preprint. Discussion started: 27 August 2024

Skamarock, W. C., Klemp, J. B., Dudhia, J., Gill, D. O., Liu, Z., Berner, J., Wang, W., Powers, J. G., Duda, M. G., Barker, D. M., and Huang, X.-Y.: A Description of the Advanced Research WRF Model Version 4, Tech. rep., NCAR Technical Note NCAR/TN-556+STR, https://doi.org/10.5065/1dfh-6p97, 2019.

Söderberg, S. and Parmhed, O.: Numerical Modelling of Katabatic Flow Over a Melting Outflow Glacier, Boundary-Layer Meteorol., 120, 509–534, https://doi.org/10.1007/s10546-006-9059-3, 2006.

Steyn, D. G., Wekker, S. F. J. D., Kossmann, M., and Martilli, A.: Boundary Layers and Air Quality in Mountainous Terrain, in: Mountain Weather Research and Forecasting, edited by Chow, F. K., De Wekker, S. F. J., and Snyder, B. J., Springer Atmospheric Sciences, pp. 261–289, Springer Netherlands, https://doi.org/10.1007/978-94-007-4098-3_5, 2013.

Strasser, U., Marke, T., Braun, L., Escher-Vetter, H., Juen, I., Kuhn, M., Maussion, F., Mayer, C., Nicholson, L., Niedertscheider, K., Sailer, R., Stötter, J., Weber, M., and Kaser, G.: The Rofental: a high Alpine research basin (1890–3770 m a.s.l.) in the Ötztal Alps (Austria) with over 150 years of hydrometeorological and glaciological observations, Earth Syst. Sci. Data, 10, 151–171, https://doi.org/10.5194/essd-10-151-2018, 2018.

Thompson, G., Field, P. R., Rasmussen, R. M., and Hall, W. D.: Explicit Forecasts of Winter Precipitation Using an Improved Bulk Microphysics Scheme. Part II: Implementation of a New Snow Parameterization, Mon. Wea. Rev., 136, 5095 – 5115, https://doi.org/10.1175/2008MWR2387.1, 2008.

Turton, J. V., Kirchgaessner, A., Ross, A. N., and King, J. C.: The spatial distribution and temporal variability of föhn winds over the Larsen C ice shelf, Antarctica, Q. J. R. Meteorol. Soc., 144, 1169–1178, https://doi.org/10.1002/qj.3284, 2018.

Umek, L.: lukasumek/WRF_LES_diagnostics: WRF_LES_diagnostics, https://doi.org/10.5281/zenodo.3901119, 2020.

Voordendag, A., Prinz, R., Schuster, L., and Kaser, G.: Brief communication: The Glacier Loss Day as an indicator of a record-breaking negative glacier mass balance in 2022, The Cryosphere, 17, 3661–3665, https://doi.org/10.5194/tc-17-3661-2023, 2023.

Voordendag, A., Goger, B., Prinz, R., Sauter, T., Mölg, T., Saigger, M., and Kaser, G.: A novel framework to investigate wind-driven snow redistribution over an Alpine glacier: combination of high-resolution terrestrial laser scans and large-eddy simulations, The Cryosphere, 18, 849–868, https://doi.org/10.5194/tc-18-849-2024, 2024.

Vosper, S. B., Ross, A. N., Renfrew, I. A., Sheridan, P., Elvidge, A. D., and Grubišić, V.: Current Challenges in Orographic Flow Dynamics: Turbulent Exchange Due to Low-Level Gravity-Wave Processes, Atmosphere, 9, https://doi.org/10.3390/atmos9090361, 2018.

Wagner, J. S., Gohm, A., and Rotach, M. W.: The Impact of Horizontal Model Grid Resolution on the Boundary Layer Structure over an Idealized Valley, Mon. Wea. Rev., 142, 3446–3465, https://doi.org/10.1175/MWR-D-14-00002.1, 2014.

WGMS: Hintereisferner, Alps, https://wgms.ch/products_ref_glaciers/hintereisferner-alps/, 2017.

Whiteman, C. D. and Doran, J. C.: The Relationship between Overlying Synoptic-Scale Flows and Winds within a Valley, J. Appl. Meteor., 32, 1669–1682, https://doi.org/10.1175/1520-0450(1993)032<1669:TRBOSS>2.0.CO;2, 1993.

Zängl, G.: The impact of weak synoptic forcing on the valley-wind circulation in the Alpine Inn Valley, Meteorol. Atmos. Phys., 105, 37–53, https://doi.org/10.1007/s00703-009-0030-y, 2009.

Zardi, D. and Whiteman, C. D.: Diurnal Mountain Wind Systems, in: Mountain Weather Research and Forecasting, edited by Chow, F. K., De Wekker, S. F. J., and Snyder, B. J., Springer Atmospheric Sciences, pp. 35–119, Springer Netherlands, https://doi.org/10.1007/978-94-007-4098-3, 2013.

Zekollari, H., Huss, M., and Farinotti, D.: Modelling the future evolution of glaciers in the European Alps under the EURO-CORDEX RCM ensemble, The Cryosphere, 13, 1125–1146, https://doi.org/10.5194/tc-13-1125-2019, 2019.